Check for updates

OPEN

Discovery of a new class of orthosteric antagonists with nanomolar potency at extrasynaptic GABA$_A$ receptors

Christina Birkedahl Falk-Petersen[1], Tsonko M. Tsonkov[1], Malene Sofie Nielsen[1], Kasper Harpsøe[1], Christoffer Bundgaard[2], Bente Frølund[1], Uffe Kristiansen[1], David E. Gloriam[1] & Petrine Wellendorph[1] ✉

Brain GABA$_A$ receptors are ionotropic receptors belonging to the class of Cys-loop receptors and are important drug targets for the treatment of anxiety and sleep disorders. By screening a compound library (2,112 compounds) at recombinant human $\alpha_4\beta_1\delta$ GABA$_A$ receptors heterologously expressed in a HEK cell line, we identified a scaffold of spirocyclic compounds with nanomolar antagonist activity at GABA$_A$ receptors. The initial screening hit 2027 (IC$_{50}$ of 1.03 μM) was used for analogue search resulting in 018 (IC$_{50}$ of 0.088 μM). 018 was most potent at $\alpha_{3,4,5}$-subunit containing receptors, thus showing preference for forebrain-expressed extrasynaptic receptors. Schild analysis of 018 at recombinant human $\alpha_4\beta_1\delta$ receptors and displacement of [^{3}H]muscimol binding in rat cortical homogenate independently confirmed a competitive profile. The antagonist profile of 018 was further validated by whole-cell patch-clamp electrophysiology, where kinetic studies revealed a slow dissociation rate and a shallow hill slope was observed. Membrane permeability studies showed that 2027 and 018 do not cross membranes, thus making the compounds less attractive for studying central GABA$_A$ receptors effects, but conversely more attractive as tool compounds in relation to emerging peripheral GABA$_A$ receptor-mediated effects of GABA e.g. in the immune system.

GABA$_A$ receptors (GABA$_A$Rs) are ligand-gated chloride channels belonging to the Cys-loop receptor family responsible for mediating the majority of inhibition in the CNS. The receptors are assembled from 19 different subunits (α1-6, β1-3, γ1-3, ρ1-3, ϵ, π and θ)[1] with distinct combinations depending on regional brain distribution, cell type and subcellular localization[2]. The predominant GABA$_A$R subtype in the forebrain is $\alpha_1\beta_2\gamma_2$ which is found at synaptic locations mediating fast synaptic inhibition[2]. This is in contrast to receptors containing the δ-subunit which are located at extrasynaptic sites and mediate tonic inhibition[3]. In forebrain regions such as thalamus and hippocampus, the δ-subunit predominantly partners with the α_4-subunit, whereas in cerebellum it exclusively partners with the α_6-subunit[4,5], in all cases forming receptors primarily found at extrasynaptic sites. $\alpha_5\beta\gamma$ receptors are also found at extrasynaptic sites[6] and, similar to the δ-containing receptors, they generally show a high affinity for GABA (activated by GABA spill-over from the synapse) and slow desensitization compared to synaptic receptors[3,7].

GABA$_A$Rs are well established drug targets, with a number of approved drugs including the anxiolytic and sleep-inducing benzodiazepines, e.g. diazepam, and anaesthetics, e.g. propofol. Over the last decades, extrasynaptic GABA$_A$Rs have been the focus of many studies as they are proposed to be involved in a number of neurological disorders including epilepsy, sleep disorders, depression and stroke where changes in the tonic inhibition seem to be part of the pathology[8–11]. $\alpha_4\beta\delta$ receptors have also been found to be important for synaptic pruning as the expression of these receptors are increased in hippocampal CA1 neurons during puberty[12]. An increase in the expression of $\alpha\beta\delta$ receptors, and hence higher levels of tonic inhibition in hippocampal CA1, has been linked to impaired synaptic plasticity, thus indicating that these receptors also play an important role under normal physiological conditions[13]. The $\alpha_5\beta\gamma_2$ receptor subtype has also been found to be important for cognition and learning[14].

[1]Department of Drug Design and Pharmacology, Faculty of Health and Medical Sciences, University of Copenhagen, Universitetsparken 2, 2100, Copenhagen Ø, Denmark. [2]Translational DMPK, H. Lundbeck A/S, Ottiliavej 9, 2500, Valby, Denmark. ✉e-mail: pw@sund.ku.dk

Receptor	2027 (IC$_{50}$ (μM), pIC$_{50}$ ± SEM, n)		018 (IC$_{50}$ (μM), pIC$_{50}$ ± SEM, n)		GABA (EC$_{50}$ (μM), pEC$_{50}$ ± SEM, n)		GABA EC$_{80}$, μM
$\alpha_1\beta_2\delta$	6.68	(5.17 ± 0.10, 3)	0.24	(6.61 ± 0.050, 4)	6.71	(5.17 ± 0.087, 4)[a]	10–14
$\alpha_1\beta_2\gamma_2$	4.96	(5.30 ± 0.17, 4)	0.79	(6.10 ± 0.11, 4)	1.71	(5.77 ± 0.022, 3)	8.0
$\alpha_2\beta_2\gamma_2$	2.96	(5.53 ± 0.19, 3)	0.32	(6.49 ± 0.13, 3)	1.47	(5.83 ± 0.045, 3)	10
$\alpha_3\beta_2\gamma_2$	0.29	(6.54 ± 0.17, 3)	0.079	(7.10 ± 0.18, 3)	2.21	(5.63 ± 0.11, 3)	10
$\alpha_4\beta_1\delta$	1.03	(5.99 ± 0.028, 3)	0.088	(7.06 ± 0.11, 4)	0.17	(6.77 ± 0.11, 3)	0.27–1.0
$\alpha_4\beta_1\gamma_2$	0.17	(6.78 ± 0.081, 3)	0.037	(7.43 ± 0.094, 3)	1.40	(5.86 ± 0.014, 3)	4.0–8.0
$\alpha_4\beta_2\delta$	0.36	(6.44 ± 0.12, 3)	0.068	(7.17 ± 0.080, 3)	0.25	(6.61 ± 0.030, 3)[a]	0.80–1.0
$\alpha_5\beta_2\gamma_2$	0.59	(6.23 ± 0.19, 4)	0.051	(7.29 ± 0.19, 4)	0.47	(6.33 ± 0.20, 3)	3.0
$\alpha_6\beta_2\delta$	4.13	(5.38 ± 0.050, 3)	0.33	(6.48 ± 0.082, 3)	0.21	(6.68 ± 0.13, 3)[a]	3.0

Table 1. Antagonist activity of **2027** and **018** plus GABA agonist potencies at selected GABA$_A$ receptor subtypes determined in the FMP assay. The antagonist activity was determined using the stated GABA EC$_{80}$ concentration calculated from the determined GABA potencies. IC$_{50}$/EC$_{50}$ values are determined from concentration response curves and given as means. [a]Data from L'Estrade et al.[49].

Altogether this posits compounds that selectively target extrasynaptic GABA$_A$Rs as interesting tool compounds and potential drug candidates.

Nonetheless, only a limited number of extrasynaptic-preferring compounds have been identified. The most renowned compound is the orthosteric agonist gaboxadol/THIP, a super-agonist at δ-containing receptors[15], which was in clinical trials for the treatment of primary insomnia, but failed[16]. Potentially, gaboxadol is having a revival as it is currently in clinical trials for the rare disorder Angelman syndrome (trial number NCT02996305) and Fragile X (trial number NCT03697161) (as Ov101)[17], underscoring the continued interest in targeting δ-containing receptors and tonic inhibitory current levels. In addition to the δ-preferring agonist, a number of positive allosteric modulators (PAMs) have been reported. These include delta selective compound 2 (DS2)[18], AA-29504[19], the flavonoid 2'MeO6MF[20,21], and neurosteroid analogues[22,23], however none of these discriminate between $\alpha_4\beta\delta$ and $\alpha_6\beta\delta$ receptors. Interestingly, no truly selective antagonists for δ-containing receptors have been identified although the competitive antagonist DPP-4-PIOL was found to be approximately 20 times more potent in inhibiting tonic over phasic currents (IC$_{50}$ of 0.87 nM) in rat slice recordings from dentate gyrus granule cells[24]. As a whole, inhibitors of extrasynaptic GABA$_A$Rs would constitute highly useful pharmacological tool compounds, and potentially be of therapeutic relevance in e.g. functional recovery after stroke and certain types of absence epilepsies[10,25].

Here we used our recently implemented cell-based assay, measuring changes in membrane potential by fluorescence[26], to search for novel $\alpha_4\beta\delta$ receptor antagonists using $\alpha_4\beta_1\delta$ GABA$_A$Rs as a model receptor to screen an in-house assembled small-molecule compound library, and report the identification of a novel class of antagonists with a clear competitive profile and preference for $\alpha_{3,4,5}$-containing extrasynaptic GABA$_A$Rs with low to mid nanomolar potency.

Results

Validation of FMP assay for compound screening.
We have previously established a FLIPR membrane potential (FMP) assay to study recombinant δ-containing GABA$_A$Rs entailing a HEK293 Flp-In cell line stably expressing the human δ-subunit which is suitable for co-transfection with any desired α/β subunits[26]. Initially, we validated the applicability of the FMP assay for efficient compound screening in 96-well microtiter plates using the human $\alpha_4\beta_1\delta$ GABA$_A$R heterologously expressed in HEK cells. This receptor was chosen as we have previously shown this system to be reliable in expressing δ-containing receptors[26]. To this end, we determined the Z'-factor, which is a statistical factor used to measure the suitability of an assay for high throughput screening[27]. An assay is regarded an excellent assay when the value of the Z'-factor is in the range of $0.5 \leq Z' < 1$, as this indicates a large separation between positive and negative controls[27]. The Z'-factor was determined to 0.68 (three independent experiments with 48 positive and negative control wells distributed evenly across the ligand plate), thus categorizing the FMP assay on $\alpha_4\beta_1\delta$ receptors as an excellent assay for screening with high sensitivity and reproducibility.

Primary screening using the FMP assay.
The compound library was screened for antagonist activity at $\alpha_4\beta_1\delta$ receptors in the FMP assay in a single concentration of 10 μM in singlicates by applying the compounds together with a concentration of GABA corresponding to GABA EC$_{80}$ (Table 1). In the primary screening, 10 compounds inhibited the GABA EC$_{80}$ signal by more than 22%, but only two compounds, compound **2027** (N-(3-(3,9-diazaspiro[5.5]undecane-3-carbonyl)phenyl)acetamide) and **2100** (1-(furan-2-ylmethyl)-N-(2-methoxyphenyl)piperidine-4-carboxamide), were able to inhibit the signal by more than 50% (Fig. 1A,B). In the following hit validation, the same 10 compounds were tested in concentrations of 100, 50 and 10 μM in triplicates, in which only **2027** showed antagonistic effect, prominent already at a concentration of 10 μM (See Supplementary Fig. S1). Thus, we went on to further characterize **2027** by making a full concentration-inhibition curve. **2027** was able to completely inhibit the GABA EC$_{80}$-induced response in a concentration-dependent manner at $\alpha_4\beta_1\delta$ receptors with an IC$_{50}$ value of 1.03 μM (Fig. 1C, Table 1). Gabazine was included as reference compound having an IC$_{50}$ value of 0.24 μM (6.61 ± 0.058), (n = 3) at $\alpha_4\beta_1\delta$ receptors (Fig. 1A,C).
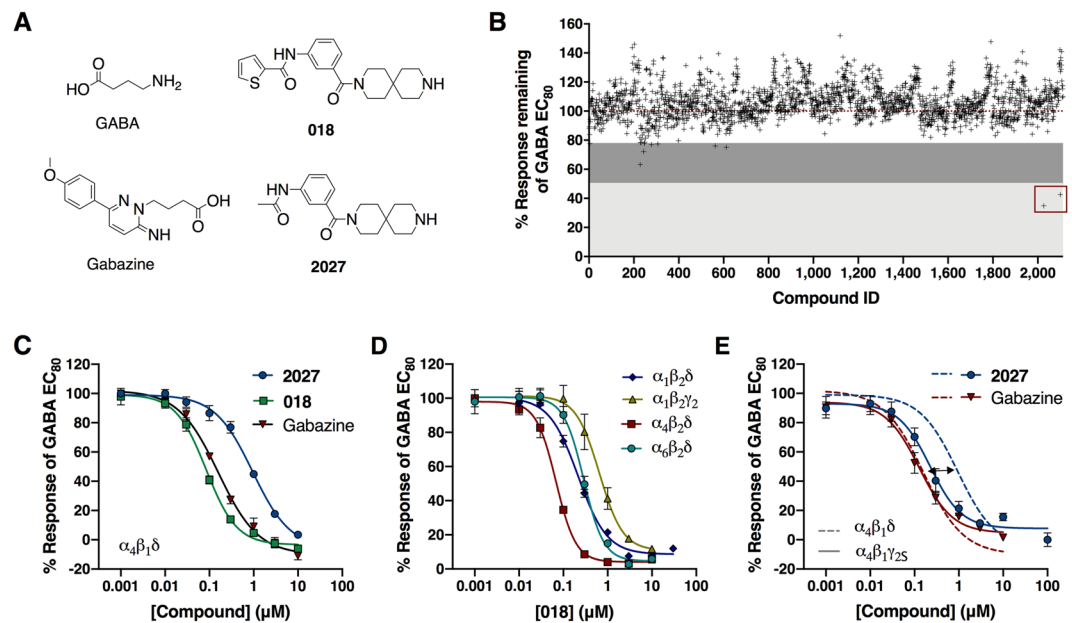
Figure 1. The identified small-molecule ligands **2027** and **018** are antagonists at $GABA_A Rs$. (**A**) Chemical structures of **018**, **2027**, GABA and Gabazine. (**B**) Results of primary screening of the compound library at $\alpha_4\beta_1\delta$ receptors in antagonist mode in the FMP assay (96-well format). Data shown are normalized to GABA EC_{80} of compounds tested in 10 μM in singlicates. (**C**) Concentration-response curves of **2027** and **018** at $\alpha_4\beta_1\delta$ receptors, with gabazine shown as reference. (**D**) Concentration-response curves of **018** at selected $GABA_A$ receptor subtypes showing α-subunit dependent inhibition of the GABA EC_{80} signal. (**E**) Concentration-response curves of **2027** and gabazine at $\alpha_4\beta_1\delta$ and $\alpha_4\beta_1\gamma_2$ showing a subtype-dependent right shift of the curve only for **2027**. Data are shown as representative curves obtained in the FMP assay with three technical replicates (means ± SD). Collected IC_{50} values ± SEM and GABA EC_{80} values are given in Table 1.

Identification of the hit analogue 018 displaying increased potency.

Next, we identified 52 structural analogues of compound **2027** by substructure searches in a database of commercially available compounds, which were tested for antagonist activity in the FMP assay in concentrations of 5 μM and 0.5 μM (For structures and data see Supplementary Figs. S2 and S3). Of the 52 analogues, 20 showed antagonist activity at 5 μM, and of these, 14 were found to be equipotent or more potent than compound **2027**. Of the 20 active analogues, **018** (*N*-(3-(3,9-diazaspiro[5.5]undecane-3-carbonyl)phenyl)thiophene-2-carboxamide) was identified as the most potent compound with an IC_{50} value of 0.09 μM at $\alpha_4\beta_1\delta$, thus being approximately 10 times more potent than **2027** (Fig. 1C, Table 1). Interestingly, all identified active compounds were found to have a common 3,9-diazaspiro[5.5]undecane moiety (Fig. 1A). Thus, based on this common structural motif, additional 44 analogues were purchased, but none of these showed to be more potent than **018** (Data not shown). We thus decided to use **018** alongside **2027** as model compounds to look further into the pharmacological properties of this new class of $GABA_A R$ antagonists.

Compound 018 shows preference for extrasynaptic $GABA_A$ receptor subtypes.

To assess if the primary hit **2027** and the more potent analogue, **018** (Fig. 1A), displayed any subtype selectivity we wanted to determine the potency at receptor subtypes in which either α, β or γ/δ subunits were interchanged. We chose subtype combinations that were both informative and physiologically relevant. Thus $\alpha_{1-3, 5}$ were expressed together with the γ_2 subunit and $\alpha_{4,6}$ with the δ-subunit[1]. Additionally, $\alpha_1\beta_2\delta$ and $\alpha_4\beta_1\gamma_2$ receptors were included, as they are relevant for comparison and found to be expressed in hippocampus[28,29]. Further, we chose to use the β_2-subunit for most receptors as it is convenient to express and because expression of β_3 leads to homomers in our cell system[26] (Table 1). First, we determined the GABA EC_{50} values at all the selected receptors in order to calculate the concentrations corresponding to GABA EC_{80}. These values are stated in Table 1, and are overall similar to values determined by others at human subtypes expressed in HEK cells[30], with GABA being more potent at the extrasynaptic and δ-containing receptors compared to γ-containing synaptic receptors. Next, we determined and compared the potencies of **2027** and **018** at the selected receptors. From these comparisons, we found that the observed potency depends most strongly on the specific α-subunit (Fig. 1D, Table 1). **018** was most potent at α_{3-5} containing receptors, with potencies in the mid nanomolar range (37–88 nM) whereas the potency at $\alpha_{1,2,6}$ receptors were in the high nanomolar range (240–790 nM). From this it follows that at a concentration of 10–100 nM, **018** would result in more than 50% inhibition of the α_{3-5} containing receptors but less than 20% inhibition at the $\alpha_{1,2,6}$ containing receptors. Comparing the potency at $\alpha_4\beta_2\delta$ receptors (IC_{50} of 68 nM) and $\alpha_1\beta_2\gamma_2$ receptors (IC_{50} of 790 nM) showed 12 times increased potency of **018** at the α_4- compared to the α_1-containing receptors. The potency ranking based on α-subunit, $\alpha_4 = \alpha_5 = \alpha_3 > \alpha_2 > \alpha_6 = \alpha_1$, indicates a preference for the forebrain extrasynaptic $GABA_A Rs$, often carrying α_4 (Fig. 1D, Table 1). Overall, a similar trend in potency order
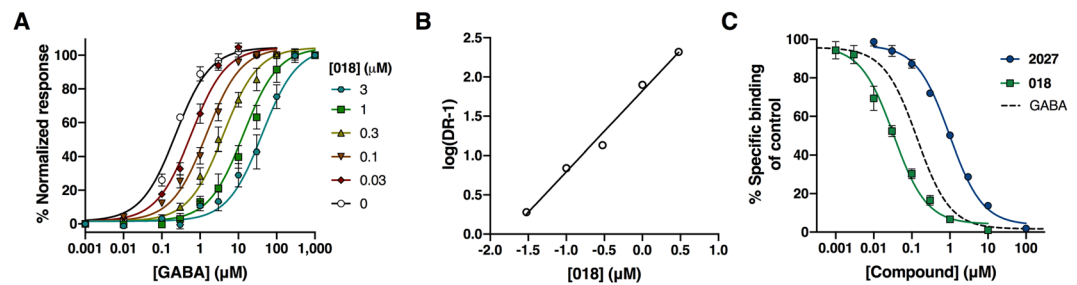
Figure 2. Compound **018** is a competitive antagonist at $\alpha_4\beta_1\delta$ receptors and displaces [^{3}H]muscimol binding. (**A**) Schild plot of **018** at $\alpha_4\beta_1\delta$ receptors determined in the FMP assay showing a right shift of the GABA concentration-response curve with increasing concentrations of **018** without affecting efficacy. Shown are pooled data from five independent experiments with three technical replicates given as means $\pm$ SEM. (**B**) Schild plot of data displayed in (**A**) showing a Schild slope of 1.03 indicative of competitive antagonism. (**C**) Concentration-dependent inhibition of [^{3}H]muscimol binding by **018** and **2027** in rat cortical homogenate, with GABA as reference, showing a competitive profile of the compounds. Data are given as means $\pm$ SEM from four independent experiments performed in technical triplicates. The K_i of GABA is 0.049 μM, data from Krall et al.[48].

was seen for **2027** albeit right-shifted 5–10 times, except for $\alpha_1\beta_2\delta$, where the potency was 28 times reduced for **2027** compared to **018** (Table 1). Finally, to assure that the observed subtype differences were not coincidental, we compared with data from the non-subtype selective antagonist, gabazine, tested at $\alpha_4\beta_1\gamma_2$ cf. $\alpha_4b_1\delta$ subtypes. As shown in Fig. 1E, gabazine has a similar IC_{50} value at both subtypes (IC_{50} of 0.11 μM (6.94 $\pm$ 0.021), n = 4 and 0.24 μM, respectively), whereas **2027**, by comparison, has a clear preference for $\alpha_4\beta_1\delta$.

Compound 018 is a competitive antagonist. To determine the type of antagonism displayed by **018**, we performed a Gaddum/Schild analysis at $\alpha_4\beta_1\delta$ receptors in the FMP assay. Thus, GABA concentration-response curves were generated in the absence or presence of increasing concentrations of **018** ranging from 0.03 μM to 3 μM. This resulted in a decrease in the potency of GABA with increasing concentrations of **018** (right-shift of curves) but without any changes in the slope and/or the efficacy of GABA at any of the tested concentrations of **018** (Fig. 2A). The Schild slope for **018** was determined to 1.03 [0.96–1.06], (n = 5) and was not significantly different from unity (P = 0.668), indicating that **018** is a competitive antagonist at $\alpha_4\beta_1\delta$ receptors (Fig. 2B). Additionally, the K_B for **018** was determined to 19 nM [0.0138; 0.0278] from the Schild analysis. To further support the finding that **018** is a competitive antagonist, its ability to inhibit radioligand binding of [^{3}H]muscimol to rat brain cortical homogenate was tested by performing competition binding studies. These experiments showed that **018** and **2027** were able to fully inhibit the binding of [^{3}H]muscimol with K_i values of 20 nM (7.71 $\pm$ 0.06), (n = 4) and 0.56 μM (6.25 $\pm$ 0.06), (n = 4), respectively (Fig. 2C). The determined K_B and K_i values correspond very well supporting a competitive profile of the compounds.

Validation using whole-cell patch-clamp electrophysiology. To validate the results from the FMP assay, compound **018** was tested in whole-cell patch-clamp electrophysiology at $\alpha_4\beta_1\delta$ receptors conveniently expressed in the same δ-HEK cell line as used for the FMP assay. Again, **018** was found to be a full antagonist and the IC_{50} value was determined to 10.8 nM [6.27; 14.7], (n = 7), which is 9 times more potent than determined in the FMP assay. The Hill slope for **018** was found to be −0.74 [−0.95; −0.54] (Fig. 3), which is more shallow than what would be expected for a competitive $GABA_AR$ antagonist[31]. To test if the shallow Hill slope was an effect of the compound or the assay, we tested the classical competitive antagonist gabazine using the same setup. The IC_{50} of gabazine was determined to 0.18 μM [0.11; 0.29], (n = 5) with a Hill slope of −1.54 [−2.2; −0.84] (Fig. 3). This is significantly steeper than that of **018** (**P = 0.0099, unpaired t-test), thus indicating that the shallow Hill slope of **018** is not a technical issue but an effect of the compound.

Compound 018 displays slow dissociation kinetics. From the patch-clamp current traces of the concentration-response curve of **018** it was apparent that the presence of **018** concentration-dependently delayed the activation phase of GABA-activated currents (Fig. 3B). For concentrations of **018** close to its IC_{50} value, it was further apparent that the activation phase followed a biphasic time course. In order to obtain detailed information on the dissociation kinetics of **018** we decided to further investigate the time-course of GABA activation in the presence of **018**. To this end, we tested concentrations of **018** ranging from 0.1 to 1000 nM pre-applied before application of 2.5 μM GABA, and determined the number of exponential components with their time constants and amplitudes that best fitted the time course of the activation phase (Fig. 4B+C, Table 2). The results show that the time course of the activation phase of the GABA currents could be described well using mono- or biexponential functions. Thus, it confirmed our initial observations, as the activation phase of the GABA current after preapplication of 3, 10 and 30 nM **018** could be fitted using biexponential functions, except for 6 of the tested cells that were fitted by mono-exponential functions (Fig. 4C, Table 2). At a concentration of 30 nM, four out of five tested cells could be fitted to both a mono- and a biexponential function, but statistical analysis showed that all were fitted best by the biexponential function (F-test, P < 0.001). The GABA activation phases with 0.1 nM and 1000 nM **018** could only be fitted using mono-exponential functions, as the slow and fast component, respectively,
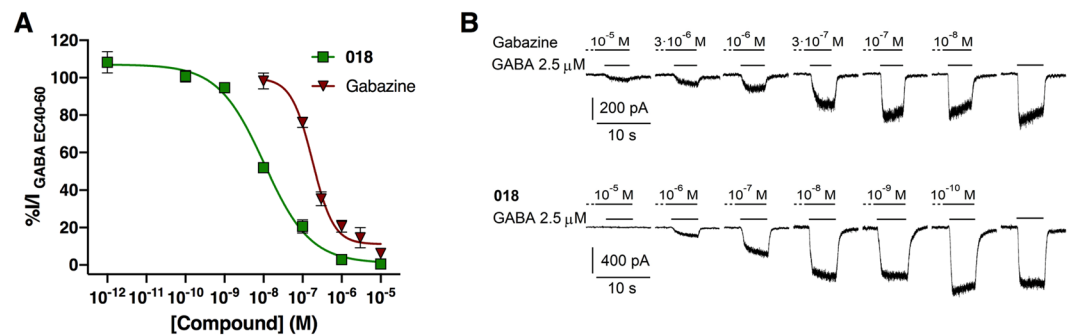
Figure 3. Whole-cell patch-clamp electrophysiology studies of $\alpha_4\beta_1\delta$ receptors support the antagonism determined in the FMP assay. (**A**) **018** concentration-dependently inhibits the current induced by 2.5 μM GABA (corresponding to GABA EC$_{30-40}$) at $\alpha_4\beta_1\delta$ receptors with an IC$_{50}$ of 10.8 nM and a Hill slope of −0.74. Gabazine was included as reference with an IC$_{50}$ of 0.18 μM and a Hill slope of −1.53. (**B**) Representative current traces for **018** and gabazine. The dotted line represents 30 sec pre-application of the antagonist. Data are shown as pooled data from 5–7 cells given as means ± SEM and normalized to the GABA 2.5 μM control.

were virtually absent at these concentrations. The determined activation time constants are given in Table 2 and Fig. 4C. The time constant for the fast component, τ_1, for 0.1–10 nM **018** was not significantly different from the single time constant, τ, for 2.5 μM GABA alone, but for 30 nM **018**, the determined τ_1 of 68.0 ms was significantly lower compared to GABA alone (P = 0.0068, Kruskal-Wallis ANOVA followed by Dunn's multiple comparison). Comparing the time constants of the slow component, τ_2, determined with the different concentrations of **018** showed that the time constant τ_2 for 3 nM **018** was significantly lower than for 1000 nM and 30 nM (P = 0.0066 and P = 0.024 respectively, Kruskal-Wallis ANOVA followed by Dunn's multiple comparison). Additional experiments using 100 μM GABA showed that the determined slow time constants, τ_2, were not significantly different from those using 2.5 μM GABA (Multiple t-test) (See Supplementary Fig. S4 and Table S1).

For those activation phases of the GABA current best fitted using a biexponential function, we determined the fraction of the total current amplitude contributed by the fast component (%A$_1$) (Fig. 4D, Table 2). For 1000 nM and 0.1 nM, which could only be fitted using mono-exponential functions (slow and fast, respectively), the %A$_1$ were set to 0% and 100%, respectively. This revealed a decrease in the relative contribution from the fast component with increasing antagonist concentrations (Fig. 4D). We interpret these observations based on the models presented in Fig. 4A, which are simple kinetic models for activation of receptors by GABA, and are based on models by Mortensen et al. and Keramidas & Harrison, for $\alpha_4\beta_3\delta$ and $\alpha_4\beta_2\delta$ receptors[32,33], respectively, assuming that $\alpha_4\beta_1\delta$ receptors display similar kinetics. Model 1 describes the activation of vacant receptors by GABA and Model 2 describes the situation when receptors are initially blocked by binding of **018**. When receptors are bound to **018**, the number of vacant receptors that GABA can activate will be reduced depending on the concentration and affinity of **018**, thus delaying the overall process of activation, with the dissociation of **018** being the rate-limiting step. Assuming that the fast component of activation is due to GABA activating the population of initially vacant receptors, it follows that the decrease in the relative contribution of the fast component (%A$_1$) with increasing antagonist concentrations (Fig. 4D) must reflect a decrease of the fraction of vacant receptors and a corresponding increase in fraction of receptors that are occupied by antagonist at the end of the pre-application.

Specifically, a %A$_1$ of 50% should correspond to a receptor occupation by **018** of 50%. The corresponding concentration of **018** is then a measure of affinity, a "functional K$_B$", provided that binding equilibrium is obtained during pre-application. In this way, the functional K$_B$ for **018** at $\alpha_4\beta_1\delta$ receptors was determined to 6.90 nM [5.99; 7.91] for 2.5 μM GABA. The same experiment was performed using 100 μM GABA giving a similar result with a functional K$_B$ of 7.80 nM [6.93; 8.73] (See Supplementary Fig. S4 and Table S1). These values concur both with the determined K$_B$ from the Schild analysis and K$_i$ from the binding studies.

018 and 2027 display very low membrane permeability.   To investigate the potential of both **018** and **2027** for *in vivo* studies, the compounds were tested in an *in vitro* permeability model using MDCK-MDR1 cells, to assess the bidirectional permeability. Results from these experiments indicate very low permeability of both **018** and **2027**. The apical to the basal permeability was 0.00 cm/s for both of the compounds whereas the basal to apical permeability was 0.79 and 0.67 10^{-6} cm/s for **018** and **2027**, respectively. Additionally, based on a high recovery both before and after (above 85%), sticking of compounds to the cells is not an issue (See Supplementary Table S2)". This indicates that the compounds most likely will not pass cell membranes and thus not get into the brain.

Discussion

We have identified a new class of competitive GABA$_A$R antagonists with preference for $\alpha_{3,4,5}$-containing extrasynaptic receptors typical in forebrain regions such as cortex, thalamus and hippocampus. Having identified **2027** as a low-micromolar GABA$_A$R antagonist, we were able to increase the potency approximately 10 times by testing of analogues with the identification of **018**. This confirmed the predictions of the library, which was designed to contain compounds that had at least 50 commercially available structural analogues, with the purpose of increasing potency of the primary hit and narrowing down the searchable chemical space.
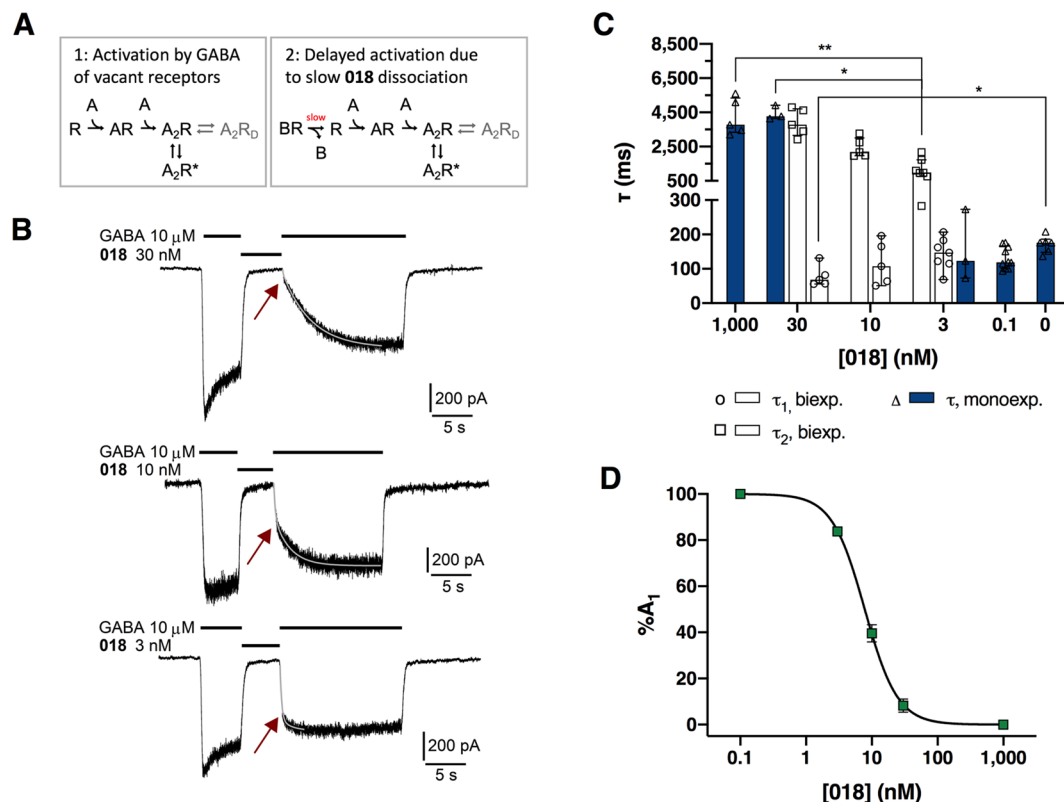
Figure 4. Compound **018** displays slow dissociation kinetics. (**A**) Simple kinetic models for the activation by GABA of vacant receptors (Model 1) and receptors initially blocked by **018** (Model 2), respectively. When present, dissociation of **018** is the slowest (rate-limiting) step and delays the overall process of activation by GABA. Openings are assumed to occur only with two agonist molecules bound (A_2R^* state) and desensitization (A_2R_D, in grey) to be of minor importance during the activation phase. (**B**) Examples of current traces for 2.5 μM GABA before and after 5 sec application of 10 nM **018** showing slow dissociation kinetics of **018**. A biexponential function (grey line) was fitted to the activation phase of the current traces, with the fast component interpreted as reflecting GABA activation of vacant receptors (Model 1), and the slow component reflecting receptors, where activation had to await dissociation of **018** (Model 2). The arrow indicates the break point where the fast component is essentially completed. (**C**) Time constants, τ, for currents induced by 2.5 μM with or without pre-application of **018**. Constants determined by fitting to a monoexponential function are shown as blue bars (Δ) and biexponential fittings in white bars ($\square, \circ$). Data are shown as median ± interquartile range for 5–10 cells. Statistical analysis was performed using Kruskal-Wallis ANOVA follow by Dunn's multiple comparison. τ_1 is compared to 0 (2.5 μM GABA without pre-application of **018**) and for τ_2 all values are compared. (**D**) The contribution from the fast-rising amplitude %A_1 concentration dependently decrease for increasing concentrations of **018** using 2.5 μM GABA, giving a functional K_B of 7.80 nM. %A_1 was determined from the fitting a to biexponential function using data displayed in (**C**). The fractional amplitude of the fast component (%A_1) is a measure of the fraction of receptors that are vacant when GABA is applied. For values see Table 2. Additional data for similar experiment using 100 μM GABA is given in supplementary Fig. S4 and Table S1.

Through the testing of analogues of **2027**, we identified the 3,9-diazaspiro[5.5]undecane moiety as an important structural element for antagonist activity. Interestingly, this structure does not contain the carboxylic acid/GABA moiety like typical orthosteric GABA$_A$R antagonists like gabazine[34] and DPP-4-PIOL[24]. It was thus interesting that the Schild analysis and binding studies of the compounds convincingly showed a competitive profile. However, there are other examples of orthosteric GABA$_A$R antagonists lacking the carboxylic acid, including bicuculline and the acid-sensing ion channel type 3 agonist 2-guanidine-4-methylquinazoline (GMQ)[35], underlining that the presence of a "GABA"-like moiety is not necessary for binding to the orthosteric site. Additionally, we found that further substitution on the secondary amine of the 3-substituted 3,9-diazaspiro[5.5]undecane structure abolished the activity of the compounds (Supplementary Figs. S2 and S3), indicating that this part of the structure is important. By comparing the structures of **018** and **2027** it is clear that there is space for rather large substituents in the 3-position of the 3,9-diazaspiro[5.5]undecane. The studies of **018** and **2027** at selected GABA$_A$ receptor subtypes showed that the α-subunit dictates potency. Comparing the IC$_{50}$ values we found that **018** is more potent at α$_{3,4,5}$-subunit containing receptors than the α$_1$-containing receptors, regardless of the presence of either the δ or γ subunit and the type of β-subunit. This conclusion could be strengthened with determination affinity-based K_B values for all subtypes. A study by Ebert et al. looked into the α-subunit selectivity of the known

018 (nM)	τ_1 (ms)	τ_2 (ms)	%A$_1$	n
0	174 [148;186][a]	—	—	6
0.1	119 [101;167][a]	—	—	10
3	147 [115;183] 123 [73.3;273][a]	1090 [960;2180] —	83.8 —	7 3
10	107 [57.5;180]	2170 [1970;3010]	39.6	5
30	68.0 [56.3;106] —	3780 [3160;4710] 4270 [4140;4920][a]	8.3 —	5 3
1000	—	3780 [3330;5350][a]	—	5

Table 2. Summary of the time constant determined for 2.5 µM GABA with and without preincubation with **018** and calculated percentage contribution of the fast-rising current (%A$_1$) relative to the total induced current. If not otherwise stated, current traces were best fitted using a biexponential function. Data are given as medians followed by 25–75% quartiles in squared brackets. n denotes the number of tested cells. Statistics are shown and described in Fig. 4B. [a]Current traces were best fitted using a monoexponential function.

competitive antagonist gabazine, bicuculline and Thio-4-PIOL at $\alpha\beta\gamma_2$ receptors, but did not find any differences between the receptor subtypes when studying functional responses[36]. It is therefore interesting that this new class of GABA$_A$R antagonists seemingly discriminate between the different α-subunits. It is however known that the GABA sensitivity is dependent on the type of α-subunit[37] which we also show here. Interestingly, there is no clear correlation between the GABA potency and those of **2027** and **018** at the different subtypes, thus underlining that the compounds might also interact with residues outside the GABA binding site that are important for the potency, e.g. via hydrophobic interactions of the distal amide and aromatic moieties assuming that the protonated 9-amino group has the same interactions as GABA and thus is located under the c-loop.

The competitive profile of **018** was corroborated by similar affinity constants obtained from the Schild analysis, radioligand binding studies, and electrophysiology, although the specific receptor subtypes present in the native membranes is not equivocal. It has previously been shown that there is good correlation between affinity and potency for GABA$_A$R antagonists[36], as shown here for both **018** and **2027**. However, as the data can be fitted to a one-site binding model, this indicates binding to either a uniform receptor population or only high-affinity δ-containing receptors because the assay protocol employed only a low nanomolar [^{3}H]muscimol concentration[38]. Immunoprecipitation studies from cortex have shown that the δ-containing receptors constitute around 10% of the total GABA$_A$Rs[39], thus only making up a small part of the available binding sites. Thus, at this point we cannot rule out that the differences observed for the α-subunits are only functional.

Patch-clamp electrophysiology studies of **018** corroborated the antagonistic profile from the FMP assay, however with a 9 times increased potency, likely relating to assay differences. Whole-cell patch-clamp is more sensitive and gives more details compared to the FMP assay, and has the advantage of measuring the response of a single cell in contrast to an average of cells in a specific well as in the FMP assay. It has previously been reported that the results between the two assays differ[18,40]. Additionally, we have also previously reported 5–8 times in potency differences of agonists between the two assays[26]. This difference however does not seem to be consistent, as the potency determined for gabazine in this study was similar in the two assays, with IC$_{50}$ values of 0.18 µM and 0.24 µM in whole-cell patch-clamp and FMP, respectively. In the FMP assay there is the potential of compounds interfering with the fluorescence which may skew responses. However, both **2027** and gabazine do not interfere with the fluorescence signals in concentrations below 10 µM, (Supplementary Fig. S5) ruling out this as a cause of the discrepancy. Additionally, we used a GABA EC$_{80}$ concentration in the FMP assay compared to GABA EC$_{40}$ in patch-clamp to avoid desensitization of the response.

From the patch-clamp experiments we observed a surprisingly shallow Hill slope for **018** compared to the classical orthosteric antagonist gabazine when using the same cells and setup. Therefore, it is more likely that the shallow Hill slope is a compound effect, which is interesting as both the Schild analysis and binding studies confirmed that the compound is competitive and thus must share or at least have an overlap with the GABA binding site. Further, it does not seem likely that the slow dissociation kinetics of the compound is the cause, as Vestergaard *et al.*[41] did not observes differences in Hill slopes for a series of analogues (competitive antagonists) of the partial GABA$_A$R agonist 4-PIOL, which included both fast and slowly dissociating antagonists. Thus, we have not been able to find an explanation for the shallow Hill slope other than being a characteristic of the compound.

The kinetics of GABA currents in the presence of **018** were studied in order to obtain additional information on the interaction of **018** with the $\alpha_4\beta_1\delta$ receptor. The observation, that the activation phase of GABA currents in the presence of **018** consisted of two exponential components, was interpreted as GABA interacting with two "populations" of receptors: those that are initially vacant and those that are initially occupied with antagonist, giving rise to the fast and slow, respectively, component of the activation phase (Fig. 4A,B). This is a simplification because, due to the reversibility and branching of the underlying processes (binding, gating, desensitization), the two populations do not remain distinct in time. Nevertheless, we found indications that the interpretation of the parameters obtained from biexponential fitting of the activation time course is indeed meaningful: First, the time constant of the fast component of activation, τ_1 (interpreted as GABA activation of vacant receptors), is similar to the time constant for activation by GABA alone, both with the high and low GABA concentration used. Second, the time constant of the slow component of activation, τ_2 (interpreted as reflecting the rate limiting antagonist dissociation), is independent of the GABA concentration and largely independent of the antagonist concentration. A trend towards faster τ_2 with lower concentrations of **018** was observed for both 100 and 2.5 µM GABA. However, this can be explained by the fact that at the lower concentrations of antagonist, the fractional

amplitude of the slow component (%A_2) is small, thus giving less reliable estimates of the τ_2. Third, the fractional amplitude of the fast component, %A_1, interpreted as the fraction of receptors that are vacant and immediately available for GABA to bind to and activate, decreases with the antagonist concentration, thus reflecting the concentration-dependent binding of **018** before application of GABA. The functional K_B obtained from this relationship is similar with both 2.5 μM and 100 μM GABA and in agreement with the K_i determined from receptor binding and the K_B from functional experiments (radioligand binding and FMP with Schild analysis). Also, the potential influence of drug application needs to be considered, since the solution exchange rate sets a limit to how fast processes can be resolved. With saturating GABA concentration, time constants as short as 35 ms were obtained, and therefore we conclude that solution exchange does not influence the slower τ values obtained in the kinetic experiments and analysis. This allows us to conclude that the time constant of the slow component of the GABA activation time course (τ_2) obtained in the presence of **018** is an estimate of the dissociation time constant of **018**. Thus, **018** is characterized as slowly dissociating with a time constant of the same order of magnitude as the most slowly dissociating GABA$_A$ antagonists described[41].

To address future *in vivo* usage of the compounds, the cellular permeability of **2027** and **018** were assessed and found to be very low, indicating that neither of these compounds will likely pass the blood-brain barrier, thus limiting their use for *in vivo* CNS studies. Nonetheless, as several studies have shown that GABA$_A$R subunits are expressed outside CNS, on for example several types of peripheral immune cells[42] and that GABA$_A$Rs can be potential targets for cancer therapy, this is not discouraging as such. For these purposes it would be an advantage to have compounds that do not get into the brain, as this will limit unwanted neurological side-effects. Thus, a compound such as **018** would be highly interesting to examine for such peripheral GABA$_A$R-mediated inhibitory effects and may have a favourable pharmacokinetic profile because of the slow dissociation kinetics. Furthermore, it would be of interest to probe the binding site further, e.g. by the development of a radiolabelled analogue, and/or computational modelling to gain more information on the binding site residues and, ultimately, the α-subunit dependence. Lastly, the $\alpha_{3,4,5}$-extrasynaptic receptor preference displayed by **018** presents an alternative, and highly desired, way to study (*in vitro*) tonic inhibition in the forebrain, e.g. by slice electrophysiology. Interestingly, the functional selectivity of the identified compounds for extrasynaptic over synaptic receptors make them promising tools, especially in the absence of δ-selective antagonist.

Methods

Materials. Dulbecco's modified Eagle medium (DMEM) containing GlutaMAX-I, foetal bovine serum (FBS), Dulbecco's phosphate-buffered saline (DPBS), penicillin-streptomycin, hygromycin B, trypsin-EDTA, and Hank's balanced salt solution (HBSS) were all purchased from Life Technologies (Paisley, UK). Polyfect transfection reagent was purchased from Qiagen (West Sussex, UK). FLIPR membrane potential Blue dye was purchased from Molecular Devices (Crawley, UK). Buffer components, poly-D-lysine (PDL) and 4-(2-hydroxyethyl)-piperazine-1-ethanesulfonic acid (HEPES) were purchased from Sigma-Aldrich (St. Louis, MO, USA). GABA and gabazine were from Tocris Bioscience (Bristol, UK). Compounds in the screening library and analogues were purchased from either Enamine, Vita-M or ChemBridge as stated in the supplementary information. [^{3}H]muscimol (36.9 Ci/mmol) was purchased from PerkinElmer (Waltham, MA, USA). Compounds **2027** and **018** can be purchased from Enamine and have ID numbers Z1839922409 and Z1839935473, respectively.

Compound design and analogue search. Starting from Enamine's > 2 million in-stock compounds, a diverse library of 2,112 compounds was designed. This library was selected for structural diversity (MolPrint2D fingerprint and Tanimoto coefficient <0.5), small drug-/lead-like size (MW 300–350), solubility (LogS > −4 and LogP < =3.5), flexibility (2–7 rotatable bonds), polarity (hydrogen bond donors + hydrogen bond acceptors + charged atoms = 3–10) and lack of reactive groups. The physicochemical properties were calculated by employing LigPrep, Epik, QikProp from Schrödinger Maestro and cxcalc form ChemAxon. To enable primary assay hits to be optimised by an 'analogue-by-catalogue' approach, we selected library compounds with at least 50 available drug-like analogues (Tanimoto coefficient > 0.55). A diversity search was conducted in the pool of screening compounds by Schrödinger Canvas (molPrint2D fingerprint and Tanimoto Coefficient = <0.5). The library was ordered ready for assaying as freeze-dried compounds in 384-well plates.

Substructure queries were constructed in MarvinSketch 17.3.27.0, 2017, ChemAxon (http://www.chemaxon.com) based on compound **2027** allowing for variations in different parts of the molecule. The actual analogue searches were performed in Instant JChem 17.2.27.0, 2017, ChemAxon (http://www.chemaxon.com) in a database of commercially available compounds combined from different vendors.

Cell culturing and transient transfection. HEK293 cells were maintained in DMEM containing GlutaMAX-I, supplemented with 10% FBS and 1% penicillin-streptomycin and incubated at 37 °C and a humidity of 5% CO_2. For expression of δ-containing GABA$_A$ receptors, a HEK293 Flp-In^{TM} cell line stably expressing the human GABA$_A$ δ-subunits (referred to as δ-HEK) was used and the γ-containing subtypes was expressed in a background HEK293 Flp-In^{TM} cell line stably expressing the G-protein coupled peptide receptor NPBWR2 (referred to as HEK background)[26], both positively selected for using 200 μg/mL hygromycin B. $\alpha_1\beta_2\gamma_2$ receptors were stably expressed in a HEK293 cell line maintained as above but with no selection (gift from Marianne L. Jensen, Neurosearch).

To express recombinant GABA$_A$ receptors human α_1, α_2, α_3, α_5, α_6, β_2, γ_2 (pcDNA3.1/Zeo) and α_4, β_1 (pUNIV)[26] subunit cDNA were transiently transfected into either δ-HEK or HEK background cells. δ-HEK cells were transfected with α- and β-subunits in a 1:1 ration whereas HEK background cells were transfected with α-, β- and γ-subunits in a 1:1:2 ratio. Human BGT1 (pcDNA5/FRT)[43] was transiently transfected into the δ-HEK cell line. δ-HEK cells transfected for whole-cell patch-clamp recordings were co-transfected with green fluorescent

protein (GFP) as well as α- and β-subunits in a 0.5:1:1 ratio (0.8 μg + 1.6 μg + 1.6 μg in a 6 cm dish) in order to identify transfected cells. The transfection was carried out using Polyfect as transfection reagent according to the manufactures protocol expect for using half the recommended volume of Polyfect.

FLIPR membrane potential (FMP) assay. The FMP assay was performed as previously described with a few modifications[26]. Briefly, HEK cells were transfected as described[26] and 16–20 hours later plated (50,000 cells/well in DMEM medium) into clear-bottomed black 96-well plates coated with poly-D-lysine and the assay performed 20–28 hours later. The assay protocol including the FMP blue dye incorporation into membranes was exactly as described in Falk-Petersen *et al.*[26]. Ligand solutions were prepared in 4x in assay buffer (HBSS supplemented with 20 mM HEPES, pH 7.4, on the day of assay supplemented with 2 mM CaCl$_2$ and 0.5 mM MgCl$_2$, which for all compounds tested for antagonism contained a concentration of GABA corresponding to approximately GABA EC$_{80}$ (given in Table 1). The ligand solutions were added to a ligand plates and incubated for 10–15 min in the FLEXstation3 plate reader (Molecular Devices, Crawley, UK) pre-heated to 37 °C. In a few cases a similarly operating machine, NOVOStar™ (BMG LABTECH GmbH, Offenburg, Germany) was used instead, giving similar results. Data was obtained as changes in fluorescence units (ΔRFU) by measuring emission at 560 nm caused by excitation at 530 nm. Unless otherwise mentioned in the text or figure legends experiments were performed in at least three independent experiments each using three technical replicates. Due to an observed edge effect for the FMP assay, outer wells were not used except for the screening. For screening results with GABA EC$_{80}$ controls giving signals of less than 60 ΔRFU in the outer wells, the compounds were retested.

Data obtained in the FMP assay are given as relative changes in fluorescence units (ΔRFU) by subtracting the average of the baseline fluorescence signal from the peak fluorescence signal after compound addition. All raw traces were inspected manually and peak signals resulting from compound/buffer addition together with signal artefacts were omitted from the analysis.

The concentration-response curves obtained in the FMP assay for both agonists (determining EC$_{50}$ values) and antagonists (determining IC$_{50}$ values) were fitted using the four-parameter concentration-response model:

$$\text{Response} = \text{bottom} + \frac{\text{top} - \text{bottom}}{1 + 10^{[(\log \text{EC}_{50} - A) \cdot n_H]}}$$

EC/IC$_{50}$ values describe the concentration resulting in the half-maximal response (halfway between top and bottom), and n$_H$ is the Hill coefficient. In order to pool the data from the individual experiments for the Schild analysis, ΔRFU were normalized to the buffer level set as 0% response and average response of the highest tested concentration of GABA was set to 100% in order to compensate for variation in the assay window between experiments. The presence of **018** did not result in a decreased plateau of the curves, as the maximum response was similar to the GABA max (100 μM) controls. Gaddum Schild analysis was performed using GraphPad Prism version 8.2.1 (GraphPad Software Inc., San Diego, CA, USA). EC$_{50}$/IC$_{50}$ values obtained in the FMP assay are given as means ± SEM from at least three independent experiments with three technical replicates, as specified in the individual figure legends.

Z′-factor determination. The Z′-factor for the FMP assay at α$_4$β$_1$δ receptors was calculated using the equation:

$$Z' = 1 - \frac{3\sigma_{c+} + 3\sigma_{c-}}{\left| \mu_{c+} - \mu_{c-} \right|}$$

with σ$_{c-}$ and σ$_{c+}$ denoting the standard deviation of the negative and positive controls, respectively, and μ$_{c+}$ and μ$_{c-}$ the means of the positive and negative controls, respectively. GABA EC$_{80}$ was the positive control and the buffer response the negative control.

Whole-cell patch-clamp electrophysiology. δ-HEK cells transiently expressing human α$_4$β$_1$δ receptors were seeded in 35 mm Petri dishes the day before experiment and used for recordings in a similar was as previously reported[26]. On the day of experiment the dishes were transferred to the stage of an Axiovert 10 microscope (Zeiss, Germany), and the culture medium was exchanged for artificial balanced salt solution (ABBS) at room temperature (20−24 °C). The ABSS solution contained the following (in mM): NaCl 140, KCl 3.5, Na$_2$HPO$_4$ 1.25, MgSO$_4$ 2, CaCl$_2$ 2, glucose 10, and HEPES 10; pH 7.35. The cells were viewed at 200× magnification, and cells containing green fluorescent protein were visualized with UV light from an HBO 50 lamp (Zeiss, Germany). The cells were approached with micropipettes of 1.2−3.3 MΩ resistance manufactured from 1.5 mm OD glass (World Precision Instruments, Sarasota, Florida) on a microelectrode puller, model PP-830 (Narishige, Tokyo, Japan). The intrapipette solution contained the following (in mM): KCl 140, MgCl$_2$ 1, CaCl$_2$ 1, EGTA 10, MgATP 2, and HEPES 10; pH 7.3. Standard patch-clamp techniques in voltage clamp mode[44] were used to record from cells in the whole-cell configuration using an EPC-9 amplifier (HEKA, Lambrecht, Germany). A clamping potential of −60 mV was used, and series resistance was 80% compensated. Whole-cell currents were recorded and subsequently analyzed using Pulse and PulseFit software (HEKA, Lambrecht, Germany).

ABSS solution containing the compounds were applied using two VC3−8xP pressurized application systems feeding into a sixteen-barreled perfusion pipette (ALA Scientific Instruments Inc., Farmingdale New York, USA) ending approximately 100 μm from the recorded cell. Between the compound applications, compound-free ABSS was applied from one of the barrels in order to quickly remove the compounds from the cell. For the concentrations-response dependent experiments, antagonist was pre-applied for 30 sec before 5 sec co-application with GABA EC$_{40}$ (2.5 μM), with 1 min intervals between the applications to let the cells fully recover. For the

kinetic studies GABA was first applied for 5 sec, followed by 5 sec application of antagonist and last 5–15 sec application of GABA, depending on when a plateau was reached. The cells were left to recover for 1 min before the next application.

For the antagonist concentration-response relationship, the equation:

$$I = \frac{I_{max}}{1 + 10^{\left[(\log IC_{50} - A)\cdot n_H\right]}}$$

was fitted to the experimental data, where I is the membrane current, A is the logarithm of the antagonist concentration, I_{max} is the maximum current that the reference agonist can induce, IC_{50} is the antagonist concentration inhibiting 50% of I_{max}, and n_H is the Hill coefficient. Data were described using means and 95% confidence intervals given en squared brackets.

Current relaxations were fitted to a single or biexponential equation using a Simplex optimization algorithm (PulseFit; HEKA, Lambrecht, Germany).

$$I(t) = I_0 + I_1 \exp\left(\frac{-t}{\tau_1}\right) + I_2 \exp\left(\frac{-t}{\tau_2}\right)$$

With I denoting the currents at a time t and τ_1 and τ_2 the time constants. All curve-fitting results were carefully inspected visually. In some cases, the current relaxations were fitted to both a mono- and a biexponential function and an *F*-test was applied to the residual sum of squares to determine the appropriateness of using a second component:

$$F = \frac{(SS_A - SS_B)df_B}{SS_B(df_A - df_B)} = \frac{(RMS_A^2 - RMS_B^2)df_B}{RMS_B^2(df_A - df_B)}$$

where SS and RMS are the sum of squares and root mean square deviation between fit and data, respectively. A and B refer to the single and biexponential fit, respectively. df represents the degree of freedom for each fit. Time constants were given as medians followed by the 25–75% percentile in square brackets. All statistical analyses performed on time constants were performed by using non-parametric tests (Kruskal-Wallis ANOVA followed by Dunn's multiple comparison), as the data do not follow a normal distribution.

All fractional amplitudes (%A) were determined from the second GABA pulse, for those concentrations of antagonist where a biexponential time course could be superimposed.

Radioligand binding assay. The binding studies were performed using rat brain homogenate prepared from the cortex of adult Sprague-Dawley male rats (250–350 g) obtained from commercial breeders (Janvier Laboratories, Le Genest-Saint-Isle, France), housed and cared for according to the Danish legislation regulating animal experiments and the European Communities Council Directive (2010/63/EU). Homogenate preparation was performed as described earlier[45]. On the day of assay, membranes stored at −20 °C was quickly thawed followed by addition of 40 volumes of ice-cold binding buffer (50 mM TRIS-HCl buffer; pH 7.4) and homogenization using and UltraTurrax homogenizer before being centrifuged at 48,000 ×*g* for 10 minutes at 4 °C. This washing procedure was repeated 4 times before the final pellet was suspended in the binding buffer to final concentration of approximately 0.5 mg/mL protein.

The radioligand binding assay was performed using [³H]muscimol in a 96-well format. [³H]muscimol (5 nM) was incubated with 75 μg/well protein with or without test compound or control at 0 °C for 1 hour in a total volume of 200 μL binding buffer in triplicates. GABA (1 mM) was used to determine non-specific binding. After incubation, the binding reaction was terminated by rapid filtration through GF/C unifilters (PerkinElmer) with the use of a 96-well Packard FilterMate cell harvester (PerkinElmer), followed by 3 times washing in 250 μL ice-cold binding buffer. After drying at 65 °C, microscintillation fluid was added to the dried filters and the radioactivity bound to the filter was quantified in a Packard TopCounter microplate scintillation counter. The obtained binding data was converted into specific binding (% of control) for each data point and fitted to the one-site competition model by linear regression (GraphPad Prism, version 8.2.1). The fitted IC_{50} values were converted into K_i values by means of the Cheng-Prusoff equation[46]. Data are from three independent experiments, performed with three technical replicates and K_i values are given as $pK_i \pm$ SEM.

Membrane permeability. Bidirectional permeability was tested for **018** and **2027** in the Madin-Darby canine kidney (MDCK) cell line expressing human multidrug resistance protein (MDR1, P-glycoprotein) (referred to as MDR1-MDCK cells) as described previously[47]. To calculate efflux ratio the permeability in the basal-to-apical direction was divided by the permeability in the apical-to-basal direction. The obtained data is from triplicate measurements.

Data analysis and statistics. Detailed descriptions of data and statistics are stated in the respective method sections. Data and statistical analysis were performed using GraphPad Prism version 8.2.1 (GraphPad software Inc., San Diego, CA, USA).

Data availability
The data generated and analysed during the present study is available from the corresponding author upon request.

References

1. Sieghart, W. & Sperk, G. Subunit composition, distribution and function of GABA$_A$ receptor subtypes. *Curr. Top. Med. Chem.* **2**, 795–816 (2002).
2. Olsen, R. W. & Sieghart, W. GABA$_A$ receptors: subtypes provide diversity of function and pharmacology. *Neuropharmacology* **56**, 141–148 (2009).
3. Farrant, M. & Nusser, Z. Variations on an inhibitory theme: phasic and tonic activation of GABA$_A$ receptors. *Nat. Rev. Neurosci.* **6**, 215–229 (2005).
4. Pirker, S., Schwarzer, C., Wieselthaler, A., Sieghart, W. & Sperk, G. GABA$_A$ receptors: immunocytochemical distribution of 13 subunits in the adult rat brain. *Neuroscience* **101**, 815–850 (2000).
5. Saxena, N. C. & Macdonald, R. L. Assembly of GABA$_A$ receptor subunits: role of the δ subunit. *J. Neurosci.* **14**, 7077–7086 (1994).
6. Semyanov, A., Walker, M. C., Kullmann, D. M. & Silver, R. A. Tonically active GABA$_A$ receptors: modulating gain and maintaining the tone. *Trends Neurosci.* **27**, 262–269 (2004).
7. Caraiscos, V. B. *et al.* Tonic inhibition in mouse hippocampal CA1 pyramidal neurons is mediated by α5 subunit-containing γ-aminobutyric acid type A receptors. *Proc. Natl. Acad. Sci. USA* **101**, 3662–3667 (2004).
8. Brickley, S. G. & Mody, I. Extrasynaptic GABA$_A$ receptors: their function in the CNS and implications for disease. *Neuron* **73**, 23–34 (2012).
9. Lie, M. E. K. *et al.* GAT3 selective substrate L-isoserine upregulates GAT3 expression and increases functional recovery after a focal ischemic stroke in mice. *J. Cereb. Blood Flow Metab.* **39**, 74–88 (2019).
10. Clarkson, A. N., Huang, B. S., MacIsaac, S. E., Mody, I. & Carmichael, S. T. Reducing excessive GABA-mediated tonic inhibition promotes functional recovery after stroke. *Nature* **468**, 305–309 (2010).
11. Mesbah-Oskui, L., Orser, B. A. & Horner, R. L. Thalamic δ-subunit containing GABA$_A$ receptors promote electrocortical signatures of deep non-REM sleep but do not mediate the effects of etomidate at the thalamus *in vivo*. *J. Neurosci.* **34**, 12253–12266 (2014).
12. Smith, S. S. α4βδ GABA$_A$ receptors and tonic inhibitory current during adolescence: effects on mood and synaptic plasticity. *Front. Neural Circuits* **7**, 1–16 (2013).
13. Whissell, P. D. *et al.* Acutely increasing δGABA$_A$ receptor activity impairs memory and inhibits synaptic plasticity in the hippocampus. *Front. Neural Circuits* **7**, 1–12 (2013).
14. Collinson, N. *et al.* Enhanced learning and memory and altered GABAergic synaptic transmission in mice lacking the α5 subunit of the GABA$_A$ receptor. *J. Neurosci.* **22**, 5572–5580 (2002).
15. Storustovu, S. I. & Ebert, B. Pharmacological characterization of agonists at δ-containing GABA$_A$ receptors: functional selectivity for extrasynaptic receptors is dependent on the absence of γ2. *J. Pharmacol. Exp. Ther.* **316**, 1351–1359 (2006).
16. Wafford, K. A. & Ebert, B. Gaboxadol - a new awakening in sleep. *Curr. Opin. Pharmacol.* **6**, 30–36 (2006).
17. Cogram, P. *et al.* Gaboxadol normalizes behavioral abnormalities in a mouse model of fragile X syndrome. *Front. Behav. Neurosci.* **13**, 1–9 (2019).
18. Wafford, K. A. *et al.* Novel compounds selectively enhance δ subunit containing GABA$_A$ receptors and increase tonic currents in thalamus. *Neuropharmacology* **56**, 182–189 (2009).
19. Vardya, I. *et al.* Positive modulation of δ-subunit containing GABA$_A$ receptors in mouse neurons. *Neuropharmacology* **63**, 469–479 (2012).
20. Karim, N. *et al.* 3-Hydroxy-2'-methoxy-6-methylflavone: a potent anxiolytic with a unique selectivity profile at GABA$_A$ receptor subtypes. *Biochem. Pharmacol.* **82**, 1971–1983 (2011).
21. Clarkson, A. N. *et al.* The flavonoid, 2'-methoxy-6-methylflavone, affords neuroprotection following focal cerebral ischaemia. *J. Cereb. Blood Flow Metab.* **39**, 1266–1282 (2019).
22. Hogenkamp, D. J. *et al.* Enaminone amides as novel orally active GABA$_A$ receptor modulators. *J. Med. Chem.* **50**, 3369–3379 (2007).
23. Johnstone, T. B. C. *et al.* Positive allosteric modulators of nonbenzodiazepine γ-aminobutyric acid$_A$ receptor subtypes for the treatment of chronic pain. *Pain* **160**, 198–209 (2019).
24. Boddum, K., Frølund, B. & Kristiansen, U. The GABA$_A$ antagonist DPP-4-PIOL selectively antagonises tonic over phasic GABAergic currents in dentate gyrus granule cells. *Neurochem. Res.* **39**, 2078–2084 (2014).
25. Cope, D. W. *et al.* Enhanced tonic GABA$_A$ inhibition in typical absence epilepsy. *Nat. Med.* **15**, 1392–1398 (2009).
26. Falk-Petersen, C. B. *et al.* Development of a robust mammalian cell-based assay for studying recombinant α4β1/3δ GABA$_A$ receptor subtypes. *Basic Clin. Pharmacol. Toxicol.* **121**, 119–129 (2017).
27. Zhang, C. & Oldenburg. A simple statistical parameter for use in evaluation and validation of high throughput screening assays. *J. Biomol. Screen.* **4**, 67–73 (1999).
28. Glykys, J. *et al.* A new naturally occurring GABA$_A$ receptor subunit partnership with high sensitivity to ethanol. *Nat. Neurosci.* **10**, 40–48 (2007).
29. Maric, D. *et al.* GABA$_A$ receptor subunit composition and functional properties of Cl⁻ channels with differential sensitivity to zolpidem in embryonic rat hippocampal cells. *J. Neurosci.* **19**, 4921–4937 (1999).
30. Mortensen, M., Patel, B. & Smart, T. G. GABA potency at GABA$_A$ receptors found in synaptic and extrasynaptic zones. *Front. Cell. Neurosci.* **6**, 1 (2012).
31. Ueno, S., Bracamontes, J., Zorumski, C., Weiss, D. S. & Steinbach, J. H. Bicuculline and gabazine are allosteric inhibitors of channel opening of the GABA$_A$ receptor. *J. Neurosci.* **17**, 625–634 (1997).
32. Mortensen, M., Ebert, B., Wafford, K. & Smart, T. G. Distinct activities of GABA agonists at synaptic- and extrasynaptic-type GABA$_A$ receptors. *J. Physiol.* **588**, 1251–1268 (2010).
33. Keramidas, A. & Harrison, N. L. Agonist-dependent single channel current and gating in α4β2δ and α1β2γ2S GABA$_A$ receptors. *J. Gen. Physiol.* **131**, 163–181 (2008).
34. Heaulme, M. *et al.* Biochemical characterization of the interaction of three pyridazinyl-GABA derivatives with the GABA$_A$ receptor site. *Brain Res.* **384**, 224–31 (1986).
35. Xiao, X., Zhu, M. X. & Xu, T. Le. 2-Guanidine-4-methylquinazoline acts as a novel competitive antagonist of A type γ-aminobutyric acid receptors. *Neuropharmacology* **75**, 126–137 (2013).
36. Ebert, B. *et al.* Differences in agonist/antagonist binding affinity and receptor transduction using recombinant human γ-aminobutyric acid type A receptors. *Mol. Pharmacol.* **52**, 1150–6 (1997).
37. Ebert, B., Wafford, K. A., Whiting, P. J., Krogsgaard-Larsen, P. & Kemp, J. A. Molecular pharmacology of γ-aminobutyric acid type A receptor agonists and partial agonists in oocytes injected with different α, β, and γ receptor subunit combinations. *Mol. Pharmacol.* **46**, 957–963 (1994).
38. Chandra, D. *et al.* Prototypic GABA$_A$ receptor agonist muscimol acts preferentially through forebrain high-affinity binding sites. *Neuropsychopharmacology* **35**, 999–1007 (2010).
39. Quirk, K., Whiting, P. J., Ian Ragan, C. & McKernan, R. M. Characterisation of δ-subunit containing GABA$_A$ receptors from rat brain. *Eur. J. Pharmacol. Mol. Pharmacol.* **290**, 175–181 (1995).
40. Pálvölgyi, A. *et al.* Loop F of the GABA$_A$ receptor alpha subunit governs GABA potency. *Neuropharmacology* **128**, 408–415 (2018).

41. Vestergaard, H. T., Cannillo, C., Frølund, B. & Kristiansen, U. Differences in kinetics of structurally related competitive GABA$_A$ receptor antagonists. *Neuropharmacology* **52**, 873–882 (2007).
42. Barragan, A., Weidner, J. M., Jin, Z., Korpi, E. R. & Birnir, B. GABAergic signalling in the immune system. *Acta Physiol.* **213**, 819–827 (2015).
43. Al-Khawaja, A. *et al.* Pharmacological identification of a guanidine-containing β-alanine analogue with low micromolar potency and selectivity for the betaine/GABA transporter 1 (BGT1). *Neurochem. Res.* **39**, 1988–1996 (2014).
44. Hamill, O. P., Marty, A., Neher, E., Sakmann, B. & Sigworth, F. J. Improved patch-clamp techniques for high-resolution current recording from cells and cell-free membrane patches. *Pflugers Arch.* **391**, 85–100 (1981).
45. Ransom, R. W. & Stec, N. L. Cooperative modulation of [^{3}H]MK-801 binding to the N-methyl-D-aspartate receptor-ion channel complex by l-glutamate, glycine, and polyamines. *J. Neurochem.* **51**, 830–836 (1988).
46. Yung-Chi, C. & Prusoff, W. H. Relationship between the inhibition constant (K_I) and the concentration of inhibitor which causes 50 per cent inhibition (I_{50}) of an enzymatic reaction. *Biochem. Pharmacol.* **22**, 3099–3108 (1973).
47. Risgaard, R. *et al.* Radiolabelling and PET brain imaging of the α$_1$-adrenoceptor antagonist Lu AE43936. *Nucl. Med. Biol.* **40**, 135–140 (2013).
48. Krall, J. *et al.* Discovery of α-substituted imidazole-4-acetic acid analogues as a novel class of ρ$_1$ γ-aminobutyric acid type A receptor antagonists with effect on retinal vascular tone. *ChemMedChem* **11**, 2299–2310 (2016).
49. L'Estrade, E. T. *et al.* Synthesis and pharmacological evaluation of [^{11}C]4-methoxy-N-[2-(thiophen-2-yl)imidazo[1,2-a]pyridin-3-yl]benzamide as a brain penetrant PET ligand selective for the δ-subunit-containing γ-aminobutyric acid type A receptors. *ACS Omega* **4**, 8846–8851 (2019).

Acknowledgements

Author contributions

C.B.F.-P. and P.W. conceived the study. T.M.T. designed the compound library under supervision from D.E.G. K.H. was responsible for selecting analogues of the screening hit. M.S.N. performed the library screening under supervision of C.B.F.-P. and P.W. C.B.F.-P. performed and analysed all pharmacological data (FMP, binding and electrophysiology studies). U.K. contributed to the design and analysis of the electrophysiology studies. B.F. provided chemistry input. C.B. performed the permeability studies. C.B.F.-P. and P.W. wrote the manuscript and all authors approved the final version.

Competing interests

The authors declare no competing interests.

Additional information

Supplementary information is available for this paper at https://doi.org/10.1038/s41598-020-66821-0.

Correspondence and requests for materials should be addressed to P.W.

Reprints and permissions information is available at www.nature.com/reprints.

Publisher's note Springer Nature remains neutral with regard to jurisdictional claims in published maps and institutional affiliations.